AIAA JOURNAL
Vol. 45, No. 2, February 2007

Using Tuned Electrical Resonance to Enhance Bang-Bang Vibration Control

Kanjuro Makihara,* Junjiro Onoda,† and Kenji Minesugi‡
Japan Aerospace Exploration Agency, Kanagawa 229-8510, Japan

DOI: 10.2514/1.21736

We enhanced the bang-bang vibration control by using an electrical resonance mechanism. The bang-bang method is used in many engineering applications because of its simplified hardware configuration in which a constant-voltage supplier is shared by multiple actuators. However, its control performance is restricted, because the supplied voltage is constant and the sharp modulation of the control input induces chattering, which wastes a significant amount of energy. Our approach to overcome these problems was to combine the bang-bang method with tuned electrical resonance. Based on an elaborate analysis of phase relations between mechanical and electrical vibrations, three switching logics were devised for the hybrid method. Experiments on a 10-bay truss structure demonstrated that our hybrid method not only enhanced vibration suppression of the bang-bang method, but also prevented control chattering.

Nomenclature

$\boldsymbol{B}_p$	=	input matrix
b_p	=	piezoelectric constant of actuator
C_p^S	=	constant-strain capacitance of actuator
$\boldsymbol{D}$	=	damping matrix
F	=	positive feedback gain
f	=	tensile force exerted on actuator
I_{rms}	=	performance measure in simulation
i	=	electric current ($\equiv -\dot{Q}$)
$\boldsymbol{K}$	=	constant-charge stiffness matrix
k_p	=	constant-charge stiffness of actuator
L	=	inductance in circuit
$\boldsymbol{M}$	=	mass matrix
Q	=	electric charge applied to actuator
R	=	resistance in circuit
$S(t)$	=	switching function (1, point 1; −1, point 2)
$\boldsymbol{u}$	=	displacement vector of all truss nodes
u_p	=	elongation of piezoelectric actuator
u_1	=	x directional displacement at tip node
V_a	=	voltage generator representing piezoelectric effect ($\equiv -b_p u_p$)
V_e	=	external voltage (greater than 0)
V_p	=	voltage applied to piezoelectric actuator
$\alpha, \beta, \gamma_1, \gamma_2$	=	positive constants
δ_{rms}	=	root mean square of displacements of all truss nodes
η_1	=	first modal displacement
ϕ	=	phase constant
ω	=	angular frequency of first modal vibration

Received 12 December 2005; revision received 28 November 2006; accepted for publication 7 November 2006.

*Aerospace Project Research Associate, Department of Space Structure and Materials, Institute of Space and Astronautical Science, 3-1-1 Yoshinodai, Sagamihara; kanjuro@svs.eng.isas.jaxa.jp. Member AIAA.

†Professor, Department of Space Structure and Materials, Institute of Space and Astronautical Science, 3-1-1 Yoshinodai, Sagamihara. Associate Fellow AIAA.

‡Associate Professor, Department of Space Structure and Materials, Institute of Space and Astronautical Science, 3-1-1 Yoshinodai, Sagamihara. Member AIAA.

I. Introduction

THERE are a large number of studies on combining piezoelectric materials and electrical devices for vibration suppression [1–3]. Piezoelectric materials possess piezoelectric and converse piezoelectric effects. The piezoelectric effect is voltage generation as a result of externally input forces or material deformation. This effect is usually exploited in sensor applications. In contrast, the converse piezoelectric effect generates forces and deforms materials as a result of input electric charges or voltages. This effect is often exploited in actuator applications. By exploiting both effects, we can convert mechanical and electrical energies back and forth between the two forms through piezoelectric materials. Piezoelectric materials are extensively used as actuators, sensors, and transducers [4–8].

A simple vibration control method using piezoelectric materials is the bang-bang active method. Because its control input has only one value that changes in polarity, multiple actuators can share one constant-voltage supplier, which simplifies hardware configuration. Another simple control method involves shunting piezoelectric materials with a circuit composed of an inductor and a resistor [9,10]. This inductive circuit has an electrical resonance that works similarly to dynamic mass dampers. We refer to this method as the passive resonance method. Regarding isolated structures for which energy sources are limited, such as space structures and sea platforms, it is imperative to simplify system configuration and minimize energy consumption. In that regard, the bang-bang active and the passive resonance methods can be used for special applications.

A number of hybrid methods combining two mechanisms have previously been proposed to enhance vibration suppression. Several active-passive hybrid piezoelectric networks (APPNs) [11–14] integrate piezoelectric materials with active energy sources and passive shunting circuits. These networks were implemented with continuously variable elements (e.g., voltage source, charge source, and variable resistance) rather than discontinuous bang-bang elements. These advanced APPNs provide satisfactory suppression performance, but at the same time, they require costly equipment. Thus, Petit et al. [15] and Makihara et al. [16] proposed hybrid methods that combine an energy-recycling semi-active approach [17–19] with the simple bang-bang active method. This energy-recycling semi-active approach has previously been analyzed from the viewpoint of energy flow [20] and used in various engineering applications [21–26], for example, a self-sensing system [23], an energy-harvesting device [24,25], and a disturbance isolator [26]. The hybrid method enhances vibration suppression of the bang-bang active method and reduces the amount of input energy that has to be supplied to the system. However, it induces chattering, due to the sharp change in piezoelectric voltage, when vibration amplitude decreases. To prevent chattering, we have to stop the vibration

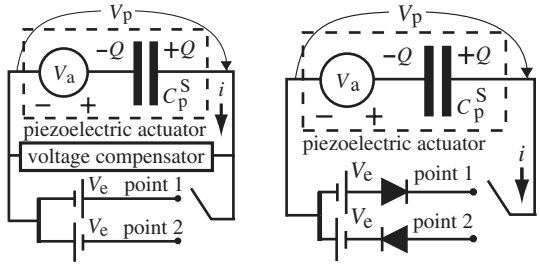

Fig. 1 Circuits for bang-bang methods: a) conventional and b) improved.

control when the vibration amplitude is small, compared with the amount of stored electrical energy [16].

II. Problem Statement

The aim of our work was to enhance vibration suppression of the bang-bang method by using an electrical resonance mechanism. Before presenting our hybrid method, we describe our improved bang-bang method and its advantages over the conventional method, because the improved bang-bang method is part of our hybrid method. The conventional bang-bang method uses the electrical circuit shown in Fig. 1a. The circuit model has a voltage supplier with a constant voltage of $V_e(>0)$ and a voltage compensator that protects against reverse flow and compensates for voltage fluctuation. Although the actual voltage supply and compensation device has a complicated electrical structure, the circuit model is simple as long as the generality of its mechanism is maintained. The piezoelectric actuator is modeled as a capacitor and a voltage generator that represents the piezoelectric effect. The voltage compensator forces piezoelectric materials to have voltages of $\pm V_e$, regardless of the voltage generated by the piezoelectric effect. In other words, the conventional bang-bang method wastes the generated voltage that would otherwise be a valuable energy source.

To make the best use of the electrical energy that the piezoelectric effect generated, we added diodes to the conventional circuit, as Fig. 1b shows. Our improved method suppresses vibration better than the conventional method, because it exploits the generated voltage instead of wasting it. Moreover, the diodes protect the voltage suppliers from damage that would otherwise be induced by electric current reversal even without a complicated voltage compensator. Thus, the first purpose of our work was to determine the advantages of our improved bang-bang method over the conventional method. Furthermore, we combined the bang-bang method with the passive resonance method. One question we needed to answer was, "What control logics work hybrid systems?" This was because the two methods comprising the hybrid method have totally different vibration suppression mechanisms. An in-depth discussion to answer this question is presented based on extensive experiments that were conducted on a 10-bay truss structure. Thus, the second purpose of our work was to determine appropriate control logics for, and to evaluate the effectiveness of, the hybrid method. Because we used the passive resonance method developed by Hagood and von Flotow [9], we focused on suppressing one dominant vibration mode, so multiple-mode vibration suppression was outside the scope of this work.

III. System Setup

This section explains the experimental setup of a truss structure with a piezoelectric actuator and presents its motion equations.

A. Experimental Setup

The 10-bay truss shown in Fig. 2a was used for the vibration suppression experiments. The total length of the truss was 3.8 m. A 0.5-kg mass was mounted at all nodes of the third and fourth bays so that frequencies of the first and second vibration modes were close together. Each axial member (i.e., longitudinal and lateral members) had an axial stiffness of 2.0×10^6 N and a length of 0.38 m. Each diagonal member had a length $\sqrt{2}$ times that of the axial member and the same axial stiffness as the axial member. The mass of each axial (diagonal) member was 36 g (46 g) and the mass of each node was 68 g. Because truss members at the base could not support the truss's total weight, the structure was hung from its tip and central nodes with strings that were 3.0-m long, as shown in Fig. 2b. The weight compensation restricted the truss's motion to the x–z plane. A displacement sensor was installed at the tip node to measure the x directional displacement. A commercially available piezoelectric actuator (NEC/TOKIN ASB171C801NP0) was installed at the truss base. The actuator had a length of 0.22 m and a mass of 93 g. The control flow was as follows (see Fig. 2b). First, the measured x directional displacement was sent to a processor. Next, the processor sent an action signal, in accordance with the switching logic, to the switch. On receiving the signal, the switch changed its connection point in the circuit.

B. Equation of Motion for Truss Structure

A piezoelectric actuator is made of multilayered piezoceramic and it generates axial force. The relation between the tensile load exerted on the actuator, elongation of the actuator, voltage, and electric charge can be written as

$$f = k_p u_p - b_p Q, \qquad V_p = -b_p u_p + Q/C_p^S \tag{1}$$

An equation of motion for the truss with the piezoelectric actuator shown in Fig. 2b can be constructed as

$$\boldsymbol{M}\ddot{\boldsymbol{u}} + \boldsymbol{D}\dot{\boldsymbol{u}} + \boldsymbol{K}\boldsymbol{u} = \boldsymbol{B}_p Q \tag{2}$$

To express Eq. (1) in vector-matrix form, we transform the scalar equation into

$$V_p = -\boldsymbol{B}_p^T \boldsymbol{u} + Q/C_p^S \tag{3}$$

Combining Eqs. (2) and (3), we obtain

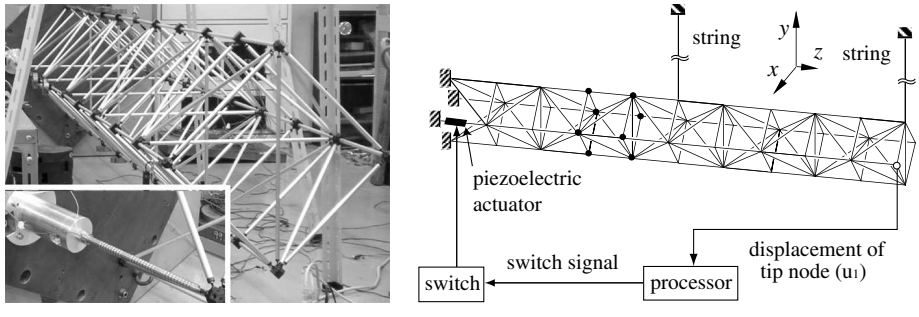

Fig. 2 Experimental setup of 10-bay truss structure: a) photographs of truss and piezoelectric actuator and b) control flow.

$$\boldsymbol{M}\ddot{\boldsymbol{u}} + \boldsymbol{D}\dot{\boldsymbol{u}} + \left(\boldsymbol{K} - C_p^S \boldsymbol{B}_p \boldsymbol{B}_p^T\right)\boldsymbol{u} = C_p^S \boldsymbol{B}_p V_p \tag{4}$$

From the direct velocity feedback control [27],

$$V_p = -F\dot{u}_p \tag{5}$$

This is a derivative control based on the time rate of change in the actuator's elongation. Because our investigation deals with only the first mode of vibration, it is possible that u_1 has the same vibration phase as u_p, for example, $u_p = \alpha u_1 (\alpha > 0)$. The active control in Eq. (5) can thus be rewritten as

$$V_p = -F\alpha\dot{u}_1 \tag{6}$$

The conventional bang-bang method has a control input voltage $V_e(>0)$ and changes only the polarity of the input. The bang-bang control logic can be expressed as

$$V_p = -V_e \mathrm{sgn}(\dot{u}_1) \tag{7}$$

where sgn( ) is the sign function.

IV. Control Designs for Vibration Suppression

We first propose an improved bang-bang method that involves adding diodes to the conventional circuit. We next describe the passive resonance method, focusing especially on the phase shift of the vibration. Based on the phase shift analysis, three possible switching logics are derived for our hybrid method.

A. Improved Bang-Bang Method

The conventional bang-bang method uses the circuit in Fig. 1a, whereas the improved method uses that in Fig. 1b. Both circuits have two voltage suppliers with constant voltages of $V_e(>0)$. Two diodes are placed in the circuit in parallel, but opposite, directions. Each is placed in the same direction as the corresponding voltage supplier. When point 1 is connected to the circuit, V_p is positive, and when point 2 is connected, V_p is negative. Following the basic control notion embodied in Eq. (7), the switching logic can be expressed as follows:

$$\begin{aligned} &\text{when } \dot{u}_1 \le 0, \quad \text{connect switch to point 1} \\ &\text{when } \dot{u}_1 > 0, \quad \text{connect switch to point 2} \end{aligned} \tag{8}$$

A suppression experiment was conducted to determine the differences between the suppression mechanisms of the improved and conventional bang-bang methods. The first mode (11.5 Hz) in the x–z plane was excited using a permanent magnet and a voice coil connected to the floor. After the excitation, the voice-coil circuit was opened so that the energy dissipating from it would not dampen the vibration of the structure. The subsequent free vibration was then suppressed with both methods. Figure 3 compares the vibration suppression performance for a supplied voltage of 1.0 V. Although the voltage was generated by the piezoelectric effect, the conventional bang-bang method always forced it to be ±1.0 V. To keep the voltage constant, we allowed the electric current to remain flowing in order to cancel out the generated voltage. Such voltage cancellation wastes a significant amount of external energy. In contrast, V_p of the improved bang-bang method was instantaneously ±1.0 V immediately after the switch connection was changed. However, after that, the magnitude of the voltage increased due to the piezoelectric effect, because the diodes prevented the electric current from flowing in the circuit so as not to decrease the voltage magnitude. Because V_p is regarded as the control input in Eq. (4), vibration suppression enhances with increasing V_p as long as the polarity of V_p is appropriate for controlling the vibration. Figure 3 shows that the improved method was more effective than the conventional method at suppressing vibration.

In summary, the conventional bang-bang method wastes valuable energy when it cancels the generated voltage. In contrast, the improved method exploits the generated voltage and is effective in vibration suppression. Furthermore, the diodes protect the voltage suppliers from damage that would otherwise be induced by reversals of the electric current, even without a complicated voltage compensator. This inherent protection is another advantage of the improved bang-bang method.

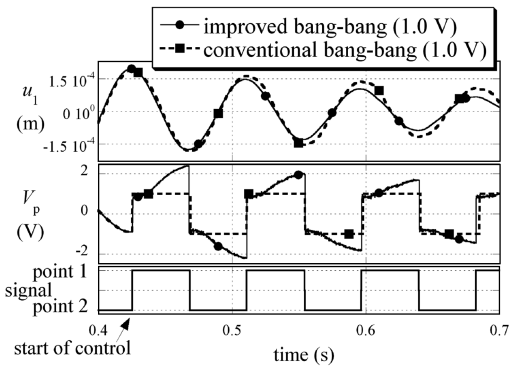

Fig. 3 Comparison of improved and conventional bang-bang methods.

B. Passive Resonance Method

Suppression experiments with the truss were conducted to investigate the suppression mechanism of the passive resonance method. The passive resonance method uses the inductive circuit (Fig. 4). The circuit had an electrical resonance coming from the inductor–capacitor combination. The electrical resonance should be tuned to the frequency of structural vibration, so it works similarly to dynamic mass dampers. In this sense, electrical parameters were determined by the process presented by Hagood and von Flotow [9]. The electrical values were $L = 1.51 \times 10^1$ H and $R = 2.37 \times 10^2\ \Omega$, as determined by an iteration process in suppression experiments. A synthetic inductor [28] composed of operational amplifiers was used. Makihara et al. [29] showed that the equivalent resistance of a piezoelectric actuator decreases with an increase in the number of cycles of the input sinusoidal voltage. We thus determined the equivalent resistance of our actuator as 3.0 Ω. The preceding resistance value ($2.37 \times 10^2\ \Omega$) included this equivalent resistance as well as circuit harnesses.

Figure 5 shows the time history of the vibration suppression experiment with the passive resonance method. The circuit switch was connected to point 4 until $t = 0.4$ s. After that, the switch was connected to point 3 so that the electric current flowed for vibration suppression. The magnitude of V_p increased after $t = 0.4$ s because of the resonance mechanism. Consequently, displacement of the truss was sufficiently suppressed within the next 0.4 s. In Fig. 5, the vibration history is divided into vibration stages 1, 2, 3, and 4. Stage 3 was intensively investigated in previous studies of the passive resonance method. Thus, we explain this vibration stage first. In stage 3, u_1 and V_p had a phase difference of $\pi/2$ (rad). In other words, V_p had the same vibration phase as $-\dot{u}_1$. It should be emphasized that this phase relation is the same as that in Eq. (6). We thus conclude that the passive resonance method inherently implements the derivative control with the $\pi/2$ phase difference. Lines B and C are drawn in the figure to indicate this phase difference. The phase difference in stage 3 is described by the following equations:

$$u_1 = \tilde{u}_1 \cos(\omega t + \phi) \tag{9}$$

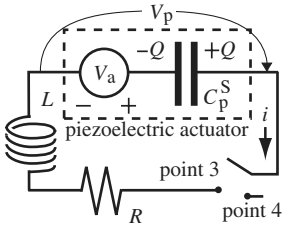

Fig. 4 Electrical circuit for the passive resonance method.

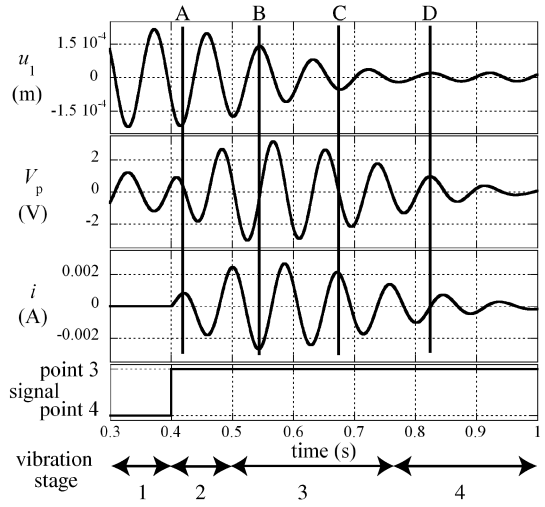

Fig. 5 Time history of vibration suppression with the passive resonance method.

$$V_p = \tilde{V}_p \cos(\omega t + \phi - \pi/2) = \tilde{V}_p \sin(\omega t + \phi) \tag{10}$$

$$i = \tilde{i} \cos(\omega t + \phi - \pi) = -\tilde{i} \cos(\omega t + \phi) \tag{11}$$

Equation (11) becomes

$$Q = \tilde{Q} \sin(\omega t + \phi) \tag{12}$$

where $\tilde{u}_1$, $\tilde{V}_p$, $\tilde{i}$, and $\tilde{Q}$ are positive functions that have much slower rates of change than sine and cosine functions having a frequency of ω.

We explain the vibration suppression mechanism of the passive resonance method by using an energy analysis. As mentioned earlier, our investigation deals with only the first modal vibration, η_1. Transforming Eq. (2) into modal coordinates and extracting the first mode, we can construct

$$\bar{m}\ddot{\eta}_1 + \bar{d}\dot{\eta}_1 + \bar{k}\eta_1 = \bar{b}Q \tag{13}$$

where $\bar{m}$, $\bar{d}$, $\bar{k}$, and $\bar{b}$ are the modal mass, damping, stiffness, and input coefficient related to the first mode; $\bar{b}$ can be positive, depending on the polarity definition of η_1. Assuming single mode vibration, it is possible that η_1 has the same vibration phase as u_1, for example, $u_1 = \beta\eta_1 (\beta > 0)$. Equation (13) then becomes

$$\bar{m}\ddot{u}_1 + \bar{d}\dot{u}_1 + \bar{k}u_1 = \gamma_1 Q \tag{14}$$

where $\gamma_1 = \bar{b}\beta (>0)$. An energy relation can thus be derived as follows:

$$\frac{\mathrm{d}}{\mathrm{d}t}\left[\frac{1}{2}\bar{m}\dot{u}_1^2 + \frac{1}{2}\bar{k}u_1^2\right] = -\bar{d}\dot{u}_1^2 + \gamma_1 Q\dot{u}_1 \tag{15}$$

The circuit with point 3 connection (Fig. 4) is represented by

$$L\dot{i} + Ri - V_p = 0 \tag{16}$$

Combining Eqs. (1) and (16), we have an energy relation as follows:

$$\frac{\mathrm{d}}{\mathrm{d}t}\left[\frac{1}{2}L\dot{Q}^2 + \frac{1}{2C_p^S}Q^2\right] = -R\dot{Q}^2 + \gamma_2 \dot{Q}u_1 \tag{17}$$

where $\gamma_2 = b_p\alpha (>0)$. By considering Eqs. (9) and (12), the phase difference between Q and $\dot{u}_1$ decreases the vibrational energy in Eq. (15). In contrast, the phase difference between $\dot{Q}$ and u_1 increases the electrical energy in Eq. (17), which increases the magnitude of Q. Equation (15) indicates that as the magnitude of Q increases, the vibrational energy decreases more rapidly. Circuits having increasing electrical energy deprive vibrating structures of more vibrational energy. Consequently, the flow from vibrational energy to electrical energy accelerates. The synergy effect between mechanical and electrical dynamics enables the passive resonance method to have an effective vibration suppression mechanism, which has been discussed in a different way in [20].

Vibration stage 1 is the state of free vibration without any control. In this stage, u_1 and V_p had a phase difference of π. This phase difference indicates that V_p was generated by u_1 because of the piezoelectric effect. Vibration stage 2 represents the duration in which the phase of V_p relative to u_1 shifts from π to $\pi/2$. As line A shows, u_1 and V_p clearly had a phase difference somewhere between $\pi/2$ and π. The phase shift was generated by strong resonance between mechanical and electrical vibrations. Vibration stage 4 indicates the free vibration state, even though the passive resonance method was still being applied. After structural vibration had been sufficiently suppressed, the phase of V_p relative to u_1 shifted to zero, as line D shows. The phase shift occurred after strong resonance vanished. Theoretically, this would not be likely to happen if the mechanical and electrical frequencies had coincided perfectly. However, a slight error was inevitable in the frequency tuning. Accordingly, the phase of V_p relative to u_1 eventually shifted to some other value, depending on the vibration history and the gap between the two frequencies. The negative effect of this phase shift on hybrid systems will be discussed later.

In previous studies of the passive resonance method [9,10], the inductive circuit connected to the piezoelectric actuator was always closed (i.e., point 3 in Fig. 4 was always connected). Therefore, previous research focused on vibration stage 3. The connection state can be altered in our hybrid system by using the switch to implement effective vibration control and prevent unnecessary consumption of external energy sources. Thus, vibration stages 2 and 4 are also important factors in determining hybrid control logics.

C. Electrical Circuit for Hybrid Vibration Suppression

Our hybrid method uses the circuit shown in Fig. 6. It is a combination of the improved bang-bang circuit (Fig. 1b) and the passive resonance circuit (Fig. 4). Points 1 and 2 are the characteristic features of this circuit. When these points are connected to the circuit, the hybrid method is implemented to suppress vibration. When point 3 is connected, the passive resonance method is implemented. Point 4 is used to disconnect the circuit. It is clear that when the switch is connected to point 1,

$$L\dot{i} + Ri - V_p = -V_e \tag{18}$$

when the switch it connected to point 2,

$$L\dot{i} + Ri - V_p = V_e \tag{19}$$

when the switch is connected to point 3,

$$L\dot{i} + Ri - V_p = 0 \tag{20}$$

when the switch is connected to point 4,

$$i = 0 \tag{21}$$

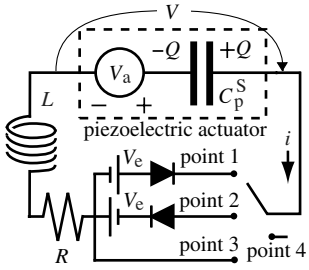

Fig. 6 Electrical circuit for hybrid vibration suppression.

D. Switching Logic for Hybrid Vibration Suppression

In this subsection, we construct switching logics for hybrid vibration suppression, by taking into account the phase shift in the passive resonance method (see Fig. 5). Because vibration stage 3 is the state for suppressing vibration, the switching logics are derived from an analysis of this vibration stage.

With the switching function, Eqs. (18) and (19) yield

$$L\dot{i} + Ri - V_p = -S(t)V_e \tag{22}$$

where $S(t) = 1$ means the connection of point 1, and $S(t) = -1$ means the connection of point 2. Equations (1) and (22) then become

$$L\ddot{Q} + R\dot{Q} + Q/C_p^S = \gamma_2 u_1 + S(t)V_e \tag{23}$$

In the same way as in Eq. (17), we obtain an energy relation as follows:

$$\frac{\mathrm{d}}{\mathrm{d}t}\left[\frac{1}{2}L\dot{Q}^2 + \frac{1}{2C_p^S}Q^2\right] = -R\dot{Q}^2 + \gamma_2 u_1\dot{Q} + S(t)V_e\dot{Q} \tag{24}$$

As explained earlier in Eq. (15), larger magnitudes of Q suppress vibration more effectively. Therefore, we intend to determine a connection point [i.e., the polarity of $S(t)$] so that electrical energy may increase as much as possible. This is the switching strategy for our hybrid vibration suppression. Note that our switching strategy is completely different from conventional vibration suppression strategies, such as decreasing total energy. In Eq. (24), $S(t)V_e\dot{Q}$ should be positive to increase electrical energy. Therefore, we obtain switching logic A as follows:

$$\begin{aligned} &\text{when } i < 0, \quad \text{connect switch to point 1} \\ &\text{when } i \geq 0, \quad \text{connect switch to point 2} \end{aligned} \tag{25}$$

Because Eqs. (9–11) indicate that u_1, $\dot{V}_p$, and $-i$ have the same vibration phase in stage 3, the following switching logics can be devised. Switching logic B is as follows:

$$\begin{aligned} &\text{when } \dot{V}_p > 0, \quad \text{connect switch to point 1} \\ &\text{when } \dot{V}_p \leq 0, \quad \text{connect switch to point 2} \end{aligned} \tag{26}$$

Switching logic C is as follows:

$$\begin{aligned} &\text{when } u_1 > 0, \quad \text{connect switch to point 1} \\ &\text{when } u_1 \leq 0, \quad \text{connect switch to point 2} \end{aligned} \tag{27}$$

Because $S(t)V_e$ is not proportional to $\ddot{Q}$ or Q in Eq. (23), the switching action does not significantly affect the electrical frequency resulting from the combination of L and C_p^S. Therefore, as will be demonstrated in the following experiments, the vibration phase relations in Eqs. (9–12) are still valid in the hybrid system.

The next section describes various aspects of the three logics. The polarity of each parameter is quite important for each switching logic, but the equality sign in each is arbitrary. The hybrid system with switching logic A cannot determine the first action of switching by itself, because the first connection point is unclear before the electric current flows (i.e., $i = 0$). Therefore, in the following experiments, we determined the first action for the hybrid system.

V. Vibration Suppression Experiment

A vibration suppression experiment was conducted to judge whether hybrid methods with switching logics A, B, and C could suppress vibration. To prevent effects from external voltages, we omitted them (i.e., $V_e = 0$) in this preliminary experiment. Figure 7 shows the time histories of vibration suppression for the passive and three hybrid methods. This figure clearly shows that the hybrid method with switching logic B did not suppress the vibration. This system could not go through vibration stage 2. Consequently, it did not arrive at stage 3, because it could not shift the phase of V_p away from π. The plots of the experimental results are arranged in the figure so that the phases of u_1 match, although control start times (i.e., times when the circuit was connected to point 2 from point 4) differ to some degree. This is because we determined the control start time of the hybrid system with switching logic A.

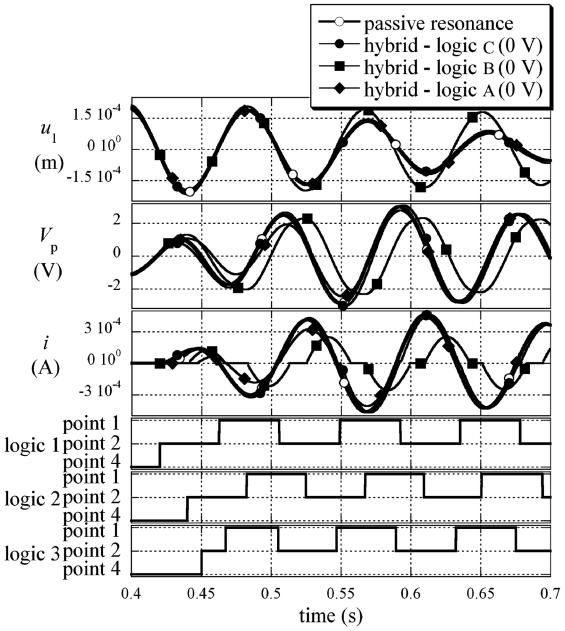

Fig. 7 Time histories of vibration suppression methods.

We carried out a suppression experiment with switching logic A. Figure 8 shows the time histories of the hybrid method with external voltages of 1.0 and 1.5 V. The higher external voltage yielded better vibration suppression until $t = 0.7$ s. However, after $t = 0.7$ s, the phase of V_p relative to u_1 deviated from $\pi/2$, and the external voltages increased the amplitude of vibration, instead of decreasing it. One interpretation of this interesting phenomenon is that after the strong resonance vanished (i.e., in stage 4), V_p and u_1 had such a phase relation that the vibration of u_1 was increased by external voltages. Therefore, it is apparent that switching logic A can lead hybrid systems into an unstable state. Thus, it must not be used for vibration suppression. This phase shift of the hybrid method with switching logic A is ascribed to the interaction between mechanical vibration and electricity.

To assess switching logic C in detail, we conducted another suppression experiment. Figure 9 shows the time histories of the hybrid method with switching logic C for external voltages of 0.2, 0.5, and 1.0 V. The larger the external voltage was, the better vibration suppression was. In conclusion, the hybrid method with switching logic C was more effective than the passive resonance method. When the vibration amplitude was sufficiently small, the hybrid control stopped automatically (e.g., around $t = 0.65$ s). This beneficial effect will be discussed next.

Figure 10 compares the time histories of the passive resonance method, the improved bang-bang method with a 1.0-V supply, and

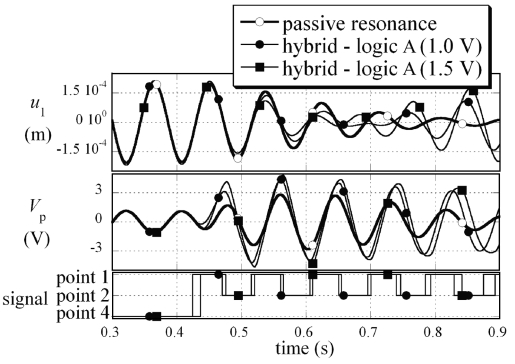

Fig. 8 Time histories of hybrid vibration suppression with switching logic A.

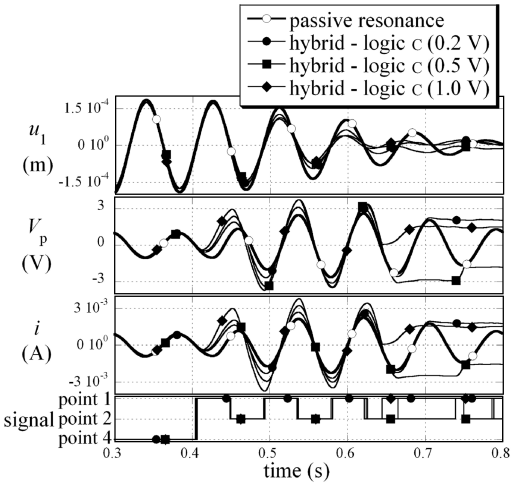

Fig. 9 Time histories of hybrid vibration suppression with switching logic C.

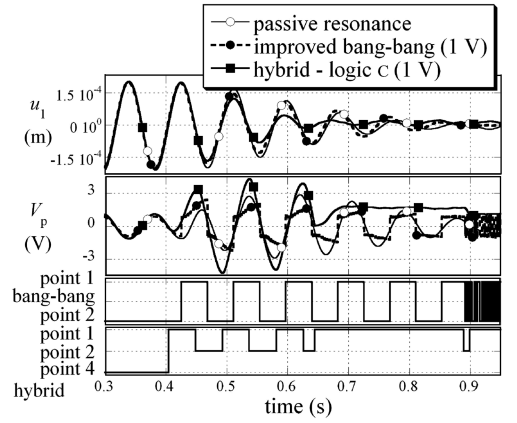

Fig. 10 Comparison of vibration suppression methods.

the hybrid method with a 1.0-V supply. First, note that the hybrid method had the best suppression performance among the three methods. Second, after $t = 0.89$ s, the bang-bang method was adversely affected by control chattering, which resulted in wasting the external voltage supply. In contrast, the hybrid and the passive resonance methods did not have chattering, because electrical inertia from large inductance prevented electrical dynamics from changing rapidly. This mechanism was quite similar to spillover prevention by inductive inertia that was previously discussed by Tang and Wang [13]. In conclusion, besides enhancing vibration suppression, the hybrid method has the advantage of inherently preventing control chattering that would degrade bang-bang vibration suppression.

A supplemental comment is presented here. Morgan and Wang [12] indicated that direct implementation of a rate feedback control law may lead to instability in APPN systems, due to the effects of circuit dynamics. Our work may provide a systematic analysis of their finding, although their variable-resistance system was different from ours and they used the time-derivative of voltage of a piezosensor.

VI. Numerical Analysis

We numerically analyzed the hybrid method's ability to suppress vibration in a 10-bay truss. This truss was the same as a model of the truss used in the suppression experiments. The values of the piezoelectric actuator model expressed in Eq. (1) were assumed to be $k_p = 5.8 \times 10^6$ N/m, $b_p = 2.6 \times 10^5$ N/C, and $C_p^S = 1.2 \times 10^{-5}$ F. The electrical values were $L = 1.51 \times 10^1$ H and $R = 2.37 \times 10^2\ \Omega$, based on the devices used in the experiments. The simulation had a time step of 1.0×10^{-7} s, which was small,

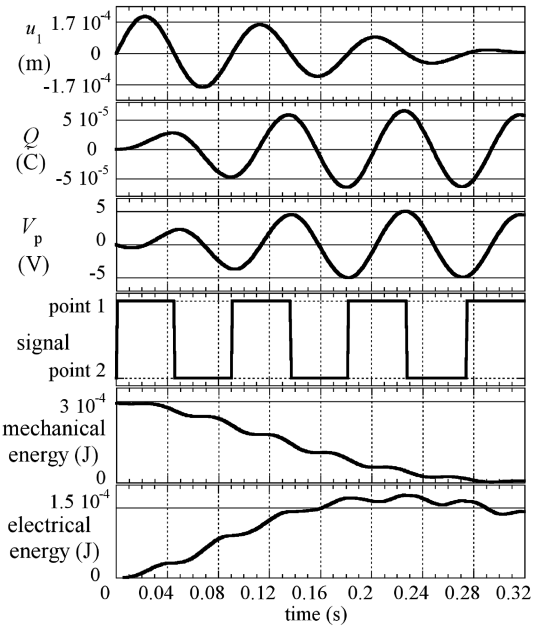

Fig. 11 Simulation of hybrid vibration suppression with switching logic C.

compared with system dynamics. We ensured that our investigation would be realistic by having the controller change its switch connection with a period of 3.0×10^{-4} s, which was the time step for the experimental hardware. The following simulations used only switching logic C for hybrid vibration suppression.

A. Energy Transition of Hybrid Vibration Suppression

Figure 11 shows the time histories of the hybrid method for an external voltage of 0.5 V. The initial modal velocity of the first mode was set to 2.5×10^{-2} m kg$^{1/2}$/s and its modal displacement was zero. The initial modal displacements and velocities of all the other modes were zero. Energy formulas were derived from the integrands in Eqs. (15) and (17), which are referred to here as mechanical and electrical energies. From the figure, we can see that the electrical energy increased, whereas the mechanical energy decreased. The hybrid method converts mechanical vibration into electrical energy as much as possible and decreases the mechanical energy rapidly. In contrast to the energy-dissipation mechanism, which is used for common vibration suppression, this energy-converting mechanism leads to significant vibration suppression, represented by the amplitude of u_1.

B. Comparison of Vibration Suppression Methods

We assessed the four suppression methods that we have discussed by varying the input value of external voltage. The following integral was calculated as a measure of vibration suppression.

$$I_{\mathrm{rms}} \equiv \int_{t_S}^{t_E} \delta_{\mathrm{rms}} \mathrm{d}t \tag{28}$$

where $t_S = 0.0$ s and $t_E = 2.0$ s. An initial velocity of $(0.1, 0.0, 0.0)$ m/s in the x–y–z coordinates was applied to the tip of the truss structure by an impulsive force (see Fig. 12). Figure 13

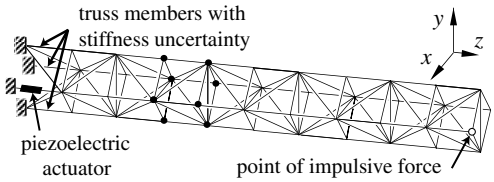

Fig. 12 Truss structure with three members having stiffness uncertainty.

plots I_{rms} for hybrid, passive resonance, and bang-bang methods, as a function of external voltage. This figure indicates that vibration suppression performances of the hybrid and the bang-bang methods depended on external voltage. When the external voltage was large, the hybrid method's performance was better than the passive resonance method's performance. When the external voltage was small, the hybrid method's performance was close to the passive resonance method's performance. The improved bang-bang method had better vibration suppression than the conventional method. These trends are quite reasonable and are consistent with our expectations.

C. Robustness Analysis of Model Errors

Regarding the passive resonance method, much attention has been paid to its vibration suppression robustness against parameter variation. Accordingly, the robustness of the hybrid method was investigated by conducting numerical simulations with intentional model errors. First, we determined the hybrid control system by selecting the optimal combination of inductance and resistance (i.e., $L = 1.51 \times 10^1$ H and $R = 2.37 \times 10^2$ Ω). Next, after determining the control system, we varied the axial stiffness EA of three truss members (see Fig. 12) by a factor of EA/EA_{nominal}, while keeping all other parameters unchanged. E is Young's modulus, and A is the cross-sectional area of the truss member. The intentional model errors were caused by this EA variation. An initial velocity of $(0.1, 0.0, 0.0)$ m/s was applied to the truss tip.

Figure 14 plots I_{rms} as a function of EA/EA_{nominal}. The slopes of the curves for the hybrid methods were shallower than that of the passive resonance method. This means that model errors did not degrade the hybrid method's performance as much as they did the passive resonance method's performance. One interpretation of this is that electrical dynamics may be slightly modified by external voltages in accordance with switching logic C that is specified with the structural dynamics (i.e., displacement, u_1), and, consequently, the mismatch between the mechanical and electrical frequencies is reduced. The vibration amplitude decreases with increasing EA/EA_{nominal}, because all systems had the same initial velocity, which explains why the plotted lines were not symmetrical with respect to the nominal line.

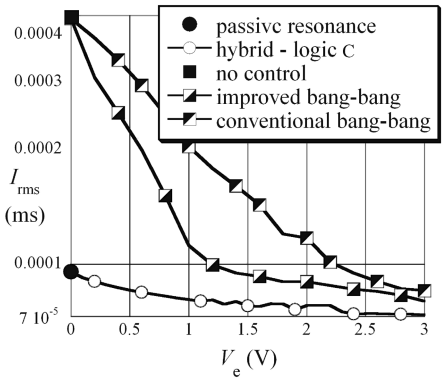

Fig. 13 Vibration suppression measure as function of external voltage.

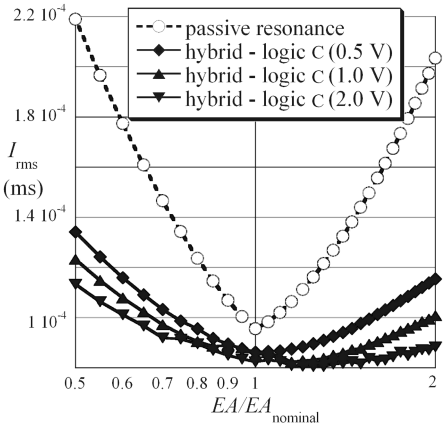

Fig. 14 Method robustness against model errors.

As mentioned earlier, for the passive resonance and the hybrid methods, the electrical resonance frequency composed of inductance L and capacitance C_p^S is tuned to the structural vibration frequency. Varying EA leads to shifts of the structural frequency, whereas electrical parameter variation leads to shifts of the electrical frequency. Therefore, both analyses based on mechanical and electrical parameter variation provide essentially the same insight into the robustness of the hybrid method. On the basis of this robustness analysis by EA variation (Fig. 14), we can thus conclude that the hybrid method is also robust against electrical frequency shift, such as by variation of L or C_p^S.

VII. Conclusions

We developed an innovative hybrid method of enhancing the bang-bang vibration control. The bang-bang method can simplify hardware configuration, because a constant-voltage supplier is shared by multiple piezoelectric actuators. However, its vibration suppression performance is limited, because the input voltage is constant and sharp modulation of its control input induces chattering, which wastes a significant amount of energy. To overcome these problems, we added an electrical resonance to the bang-bang control circuit. Three switching logics were devised on the basis of phase shift and energy flow analyses.

We determined the effectiveness of our hybrid method in experiments on a 10-bay truss structure. The investigation revealed that only one switching logic among three possible logics effectively suppressed the vibration. The hybrid method not only enhanced vibration suppression, but also prevented control chattering. Numerical simulations demonstrated that the hybrid method has an energy-converting mechanism, in contrast to the energy-dissipating mechanism that is commonly used for vibration suppression. The hybrid method was shown to be more robust against model errors than the conventional passive resonance method.

As described in this paper, the circuit switch controls the flow between mechanical and electrical energies as well as electric current. Conventional vibration controls have been based on hackneyed control strategies; they simply decreased total energy and Lyapunov function values as much as possible. In contrast, our switching control is based on energy flow and has a sophisticated control strategy, such as increasing the energy in a part of the system in order to decrease the energy in other essential parts. We believe that our sophisticated switching control based on energy flow paves the way for a new vibration control design.

Acknowledgment

This research was supported by a Grant-in-Aid for Scientific Research (B), no. 16360429, from the Japan Society for the Promotion of Science.

References

[1] Lesieutre, G., "Vibration Damping and Control Using Shunted Piezoelectric Materials," *Shock and Vibration Digest*, Vol. 30, No. 3, 1998, pp. 187–195.

[2] Giurgiutiu, V., "Review of Smart-Materials Actuation Solutions of Aeroelastic and Vibration Control," *Journal of Intelligent Material Systems and Structures*, Vol. 11, No. 7, 2000, pp. 525–544.

[3] Ahmadian, M., and DeGuilio, A. P., "Recent Advances in the Use of Piezoceramics for Vibration Suppression," *Shock and Vibration Digest*, Vol. 33, No. 1, 2001, pp. 15–22.

[4] Richard, C., Guyomar, D., and Audigier, D.,"Semi-Passive Damping Using Continuous Switching of a Piezoelectric Device," *Smart Structures and Materials 1999*, Vol. 3672, International Society for Optical Engineering, Bellingham, WA, 1999, pp. 104–111.

[5] Clark, W. W., "Vibration Control with State-Switched Piezoelectric Materials," *Journal of Intelligent Material Systems and Structures*, Vol. 11, No. 11, 2000, pp. 263–271.

[6] Niezrecki, C., Brei, D., Balakrishnan, S., and Moskalik, A., "Piezoelectric Actuation: State of the Art," *Shock and Vibration Digest*, Vol. 33, No. 4, 2001, pp. 269–280.
[7] Larson, G. D., and Cunefare, K. A., "Quarter-Cycle Switching Control for Switch-Shunted Dampers," *Journal of Vibration and Acoustics*, Vol. 126, No. 2, 2004, pp. 278–283.
[8] Sodano, H. A., Inman, D. J., and Park, G., "A Review of Power Harvesting from Vibration Using Piezoelectric Materials," *Shock and Vibration Digest*, Vol. 36, No. 3, 2004, pp. 197–205.
[9] Hagood, N. W., and von Flotow, A., "Damping of Structural Vibrations with Piezoelectric Materials and Passive Electrical Networks," *Journal of Sound and Vibration*, Vol. 146, No. 2, 1991, pp. 243–268.
[10] Wu, S., "Piezoelectric Shunts with a Parallel R-L Circuit for Structural Damping and Vibration Control," *Smart Structures and Materials 1996*, Vol. 2720, International Society for Optical Engineering, Bellingham, WA, 1996, pp. 259–269.
[11] Tsai, M. S., and Wang, K. W., "Control of a Ring Structure with Multiple Active-Passive Hybrid Piezoelectric Networks," *Smart Materials and Structures*, Vol. 5, No. 5, 1996, pp. 695–703.
[12] Morgan, R. A., and Wang, K. W., "An Integrated Active-Parametric Control Approach for Active-Passive Hybrid Piezoelectric Network with Variable Resistance," *Journal of Intelligent Material Systems and Structures*, Vol. 9, No. 7, 1998, pp. 564–573.
[13] Tang, J., and Wang, K. W., "Active-Passive Hybrid Piezoelectric Networks for Vibration Control: Comparisons and Improvement," *Smart Materials and Structures*, Vol. 10, No. 4, 2001, pp. 794–806.
[14] Morgan, R. A., and Wang, K. W., "Active-Passive Piezoelectric Absorber for Systems Under Multiple Non-Stationary Harmonic Excitation," *Journal of Sound and Vibration*, Vol. 255, No. 4, 2002, pp. 685–700.
[15] Petit, L., Lefeuvre, E., Richard, C., and Guyomar, D., "A Broadband Semi Passive Piezoelectric Technique for Structural Damping," *Smart Structures and Materials 2003*, Vol. 5386, International Society for Optical Engineering, Bellingham, WA, 2003, pp. 414–425.
[16] Makihara, K., Onoda, J., and Minesugi, K., "Low-Energy-Consumption Hybrid Vibration Suppression Based on an Energy-Recycling Approach," *AIAA Journal*, Vol. 43, No. 8, 2005, pp. 1706–1715.
[17] Richard, C., Guyomar, D., Audigier, D., and Bassaler, H., "Enhanced Semi Passive Damping using Continuous Switching of a Piezoelectric Device on an Inductor," *Smart Structures and Materials 2000*, Vol. 3989, International Society for Optical Engineering, Bellingham, WA, 2000, pp. 288–299.
[18] Corr, L. R., and Clark, W. W., "Comparison of Low Frequency Piezoceramic Shunt Techniques for Structural Damping," *Smart Structures and Materials 2001*, Vol. 4331, International Society for Optical Engineering, Bellingham, WA, 2001, pp. 262–272.
[19] Onoda, J., Makihara, K., and Minesugi, K., "Energy-Recycling Semi-Active Method for Vibration Suppression with Piezoelectric Transducers," *AIAA Journal*, Vol. 41, No. 4, 2003, pp. 711–719.
[20] Makihara, K., Onoda, J., and Minesugi, K., "Comprehensive Assessment of Semi-Active Vibration Suppression Including Energy Analysis," *Journal of Vibration and Acoustics* (to be published).
[21] Corr, L. R., and Clark, W. W., "Comparison of Low-Frequency Piezoelectric Switching Shunt Techniques for Structural Damping," *Smart Materials and Structures*, Vol. 11, No. 3, 2002, pp. 370–376.
[22] Corr, L. R., and Clark, W. W., "A Novel Semi-Active Multi-Modal Vibration Control Law for a Piezoceramic Actuator," *Journal of Vibration and Acoustics*, Vol. 125, No. 2, 2003, pp. 214–222.
[23] Makihara, K., Onoda, J., and Minesugi, K., "Novel Approach to Self-Sensing Actuation for Semi-Active Vibration Suppression," *AIAA Journal*, Vol. 44, No. 7, 2006, pp. 1445–1453.
[24] Badel, A., Guyomar, D., Lefeuvre, E., and Richard, C., "Efficiency Enhancement of a Piezoelectric Energy Harvesting Device in Pulsed Operation by Synchronous Charge Inversion," *Journal of Intelligent Material Systems and Structures*, Vol. 16, No. 10, 2005, pp. 889–901.
[25] Makihara, K., Onoda, J., and Miyakawa, T., "Low Energy Dissipation Electric Circuit for Energy-Harvesting Method," *Smart Materials and Structures*, Vol. 15, No. 5, 2006, pp. 1493–1498.
[26] Makihara, K., Onoda, J., and Minesugi, K., "New Approach to Semi-Active Vibration Isolation to Improve the Pointing Performance of Observation Satellites," *Smart Materials and Structures*, Vol. 15, No. 2, 2006, pp. 342–350.
[27] Balas, M. J., "Direct Velocity Feedback Control of Large Space Structures," *Journal of Guidance, Control, and Dynamics*, Vol. 2, No. 3, 1979, pp. 252–253.
[28] Edberg, D. L., Bicos, A. S., Fuller, C. M., Taracy, J. J., and Fechter, J. S., "Theoretical and Experimental Studies of a Truss Incorporating Active Members," *Journal of Intelligent Material Systems and Structures*, Vol. 3, No. 2, 1992, pp. 333–347.
[29] Makihara, K., Onoda, J., and Minesugi, K., "Behavior of Piezoelectric Transducer on Energy-Recycling Semi-Active Vibration Suppression," *AIAA Journal*, Vol. 44, No. 2, 2006, pp. 411–413.

C. Pierre
Associate Editor